

Daily Science Report
Stratus2007 Cruise
NOAA Ship Ronald H. Brown
C. W. Fairall (NOAA/ESRL) and R. A. Weller (WHOI)
Report #3 October 20, 2007

Summary of Recent Activities

The ship departed Panama as planned the morning of October 16. Observations were officially begun on October 18. The ship reached 12 S 79 W by the end of October 20 (Fig. 1). The ESRL observations include air-sea fluxes/near-surface bulk meteorology, cloud ceilometers, radar wind profiler, scanning Doppler C-band precipitation radar, a microwave radiometer for column water vapor/liquid, and aerosols in the 0.1 to 6 micrometer range. Rawinsonde launches are currently every 6 hours until reaching the buoy location at 20 S 85 W when the frequency will increase to every 4 hours. A sample rawinsonde profile is shown in Fig. 2; a strong subsidence inversion typical of stratocumulus regions is visible at a height of about 600 m. The trace indicates a cloud about 300 m thick. Fig. 3 is a photograph taken later in the day. The cloud ceilometer return for the day is shown in Fig. 4. At the end of this day cloud base has risen to about 600 m. The net heat flux into the ocean is about 120 W/m² (Fig. 5).

Data from the aerosol system are shown in Fig. 6. In this case we show data from the harbor in Charleston (JDs 279-283), the transect of the Gulf of Mexico and Caribbean (JDs 285-289), and the transect from the Gulf of Panama to 12 S (290-294). Note the lowest aerosol concentrations in the precipitation region of the Gulf of Panama and the highest in Charleston. Values off Peru (about 200/cm³) are typical of larger values usually found at the WHOI buoy site. So far, none of the very low values associated with pockets of open cells (POCs) have been observed.

Major activities include preparations for the DART/Tsunami buoy deployment and work on a report of findings in the Ecuador/Peru coastal region. Other activities include a launch of a drifter buoys at 1220 and 2320 GMT. A solar and longwave radiometer intercomparison project was started shortly after leaving Charleston and will continue throughout the cruise. See below for a preliminary report.

The ship will continue underway SSE for about another day before reaching the SHOA tsunami buoy at 20 S 75 W (est. 1300 on 10/22/2007).

Preliminary radiometer comparisons – Stratus-8

Contributed by E.F. Bradley

As indicated above (Figure 5), the values of long and short-wave radiation are important components of the air-sea energy transfer. For almost two decades, efforts have been made to improve the accuracy with which both of these variables may be measured. With

a nominal goal for accuracy of the ocean heat balance set at 10 Wm^{-2} over weekly to monthly timescales, we need to measure individual components to just a “few” Wm^2 . Confidence in the instrument calibration facilities and procedures is key. On the forward 02 deck of the Brown we have assembled perhaps the largest number and variety of longwave (5) and short-wave (7) radiation instruments ever on a ship for inter-comparison at sea. In particular, we aim to compare the performance of both long- and short-wave instruments from two major manufacturers. We also have a unique instrument which is purported to determine both direct and diffuse components of the global shortwave radiation.

Data management from so many different sources has been a major challenge, and has occupied much of the past few days. We now have software to assemble daily 1-minute data in a uniform format, for analysis and display. Our present situation under a complete cover of stratus cloud is not ideal for the observation of solar radiation, but a preliminary analysis of data from a fairly clear day during the transit from Charleston to Panama gives us some indication of the effects we have to examine. Figure 7 is an overplot of 4 of the 5 longwave instruments. Three of them, including two different designs, track within about 3 Wm^{-2} of one another, while the 4th is clearly apart (although by an amount which would have been regarded as cause for celebration only a few years ago). However the source of the difference (if it persists) and reasons for the slight change at daybreak (a solar trace is shown) will be of great interest. Figure 8 shows the comparison of 6 shortwave radiometers. Here the spread, seen best at the steady period around 287.6 on the time axis, is around 50 Wm^{-2} at a radiation of 700 Wm^{-2} . This is a serious discrepancy. Instruments from the two manufacturers are at opposite ends of the spread, suggesting differences in their calibration facilities.

Figure 9 shows the result of a crude test of the performance of the instrument with both total and diffuse outputs. It is mounted alongside one of our usual shortwave radiometers, and the total radiation from the two agrees extremely well. During three fairly clear periods on this day, the regular instrument was shaded with a hand-held disc to exclude the direct beam, and obtain only the diffuse component. The test involved 5 minutes shaded followed by 5 minutes clear, performed several times. The agreement is impressive. There were also a few periods when dark clouds covered the sun, and again the diffuse signal from the regular radiometer agreed well with the diffuse output from the new instrument.

The results so far are intriguing but inconclusive. This intercomparison will continue throughout the cruise. The large range of the cruise (from tropics to subtropics) will provide a good spread of conditions.

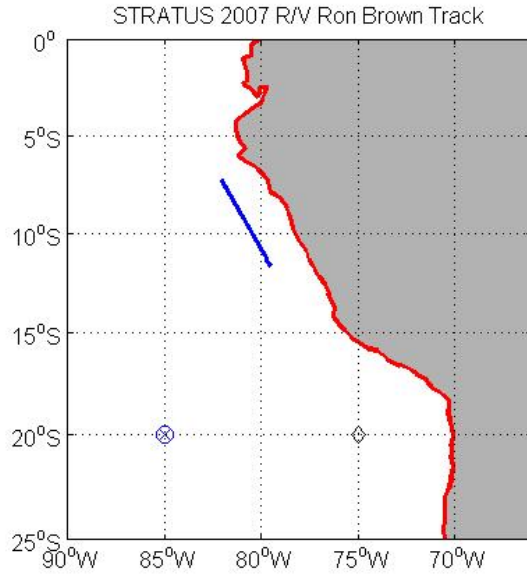


Figure 1. RHB cruise track on JD293 (Oct. 20). The diamond at 75 W is the SHOA tsunami buoy; the circle/plus at 85 W is the WHOI buoy.

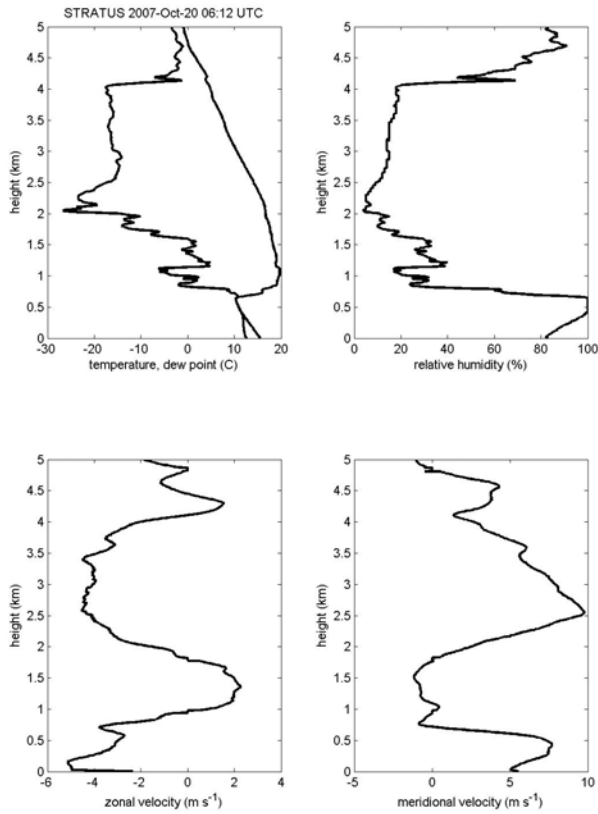


Figure 2. Rawinsonde profile 0600 GMT October 20.



Figure 3. Photograph of stratocumulus clouds 1800 GMT October 20 at 11 S 80 W.

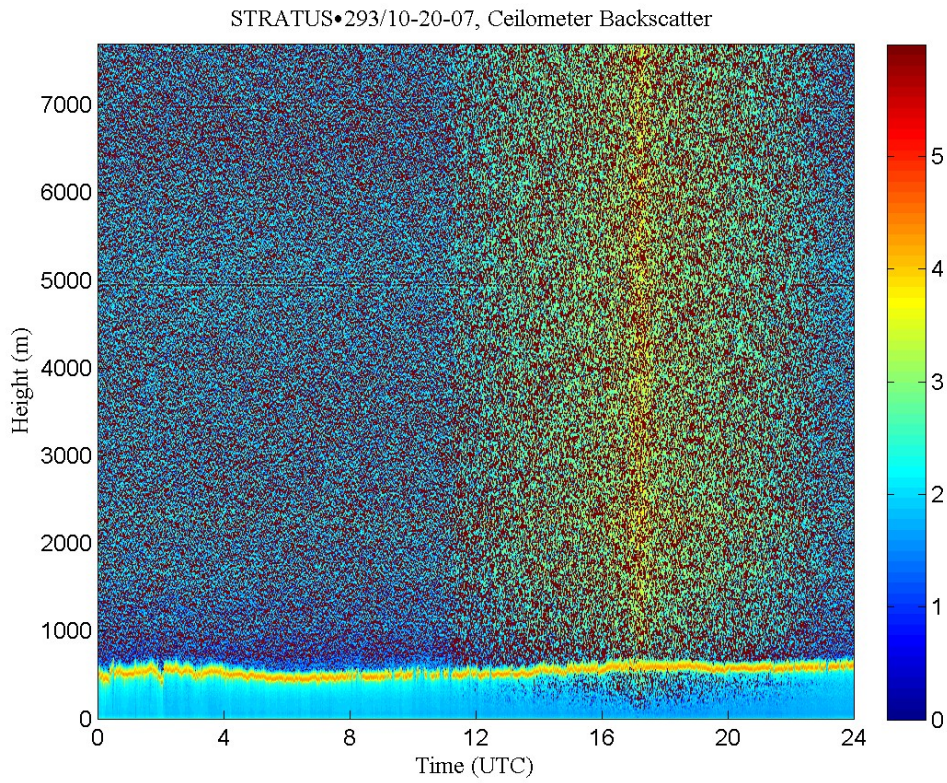


Figure 4. Time height cross section of ceilometer backscatter signal for October 20.

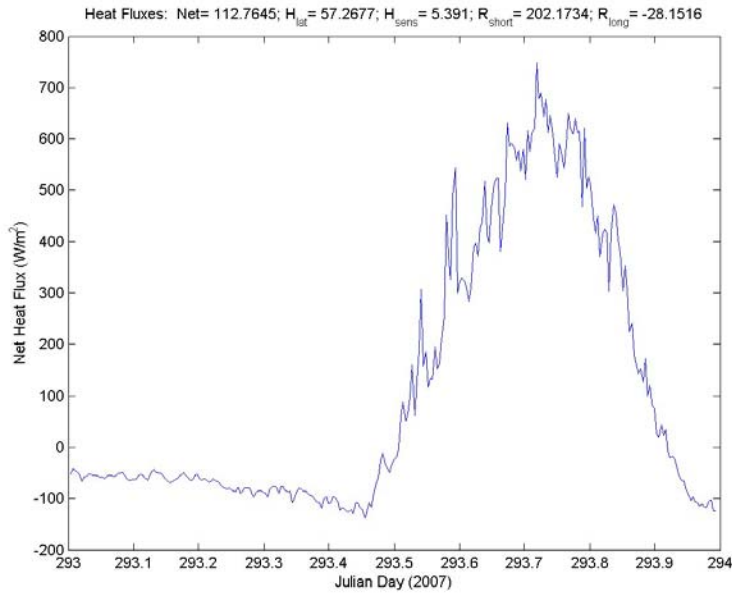


Figure 5. Time series of net heat flux into the ocean off Peru for October 20. The net heat flux is the sum of sensible (H_{sens}), Latent (H_{lat}) turbulent fluxes and net longwave (R_{long}) and net solar (R_{short}) radiative fluxes. Mean values for the day are given at the top of the graph.

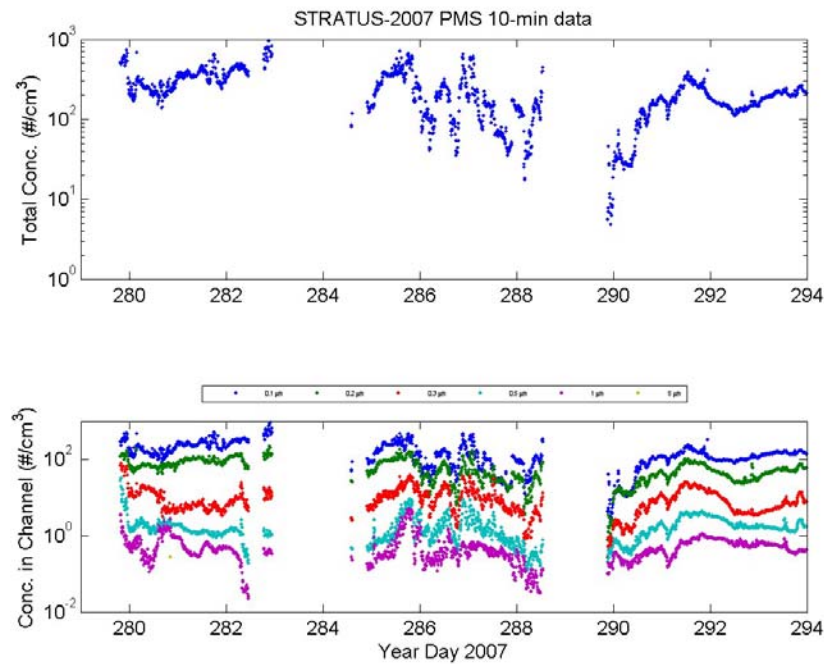


Figure 6. Time series of aerosol concentrations from Oct 6 through October 20. Upper panel: Total concentration for sizes from 0.1 to 5 micrometer. Lower panel: size resolved concentrations.

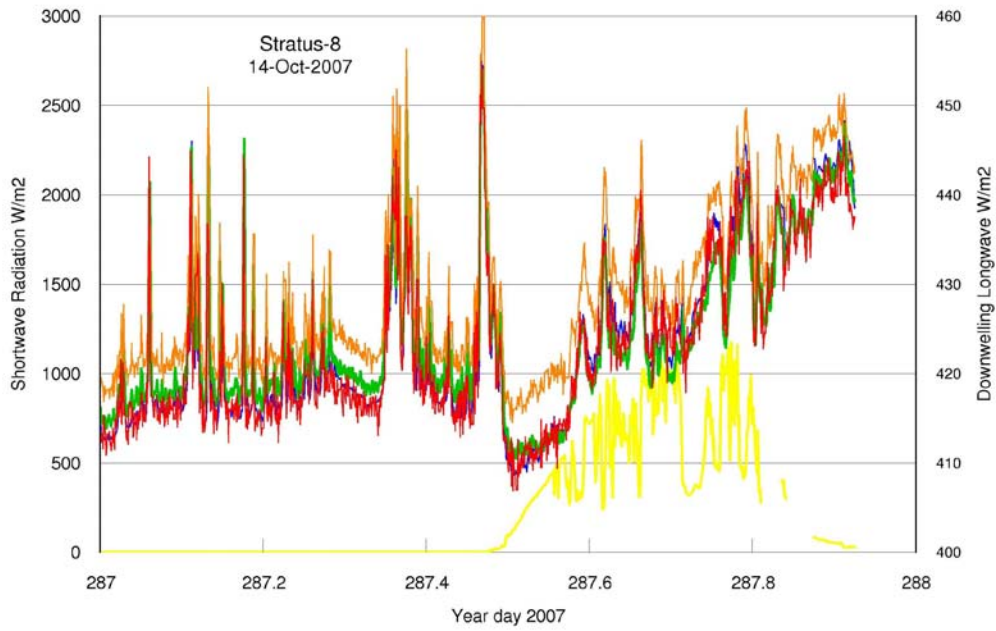


Figure 7. Time series of downward IR flux from 4 pyrgeometers (right hand scale). The yellow trace is solar flux (left hand scale).

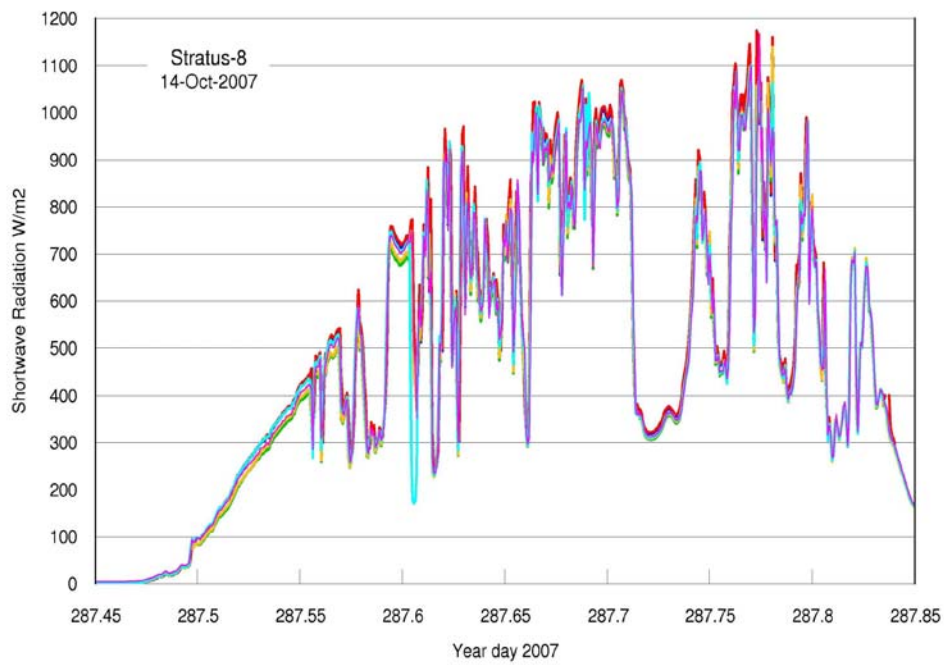


Figure 8. Time series of downward solar flux from 6 pyranometers.

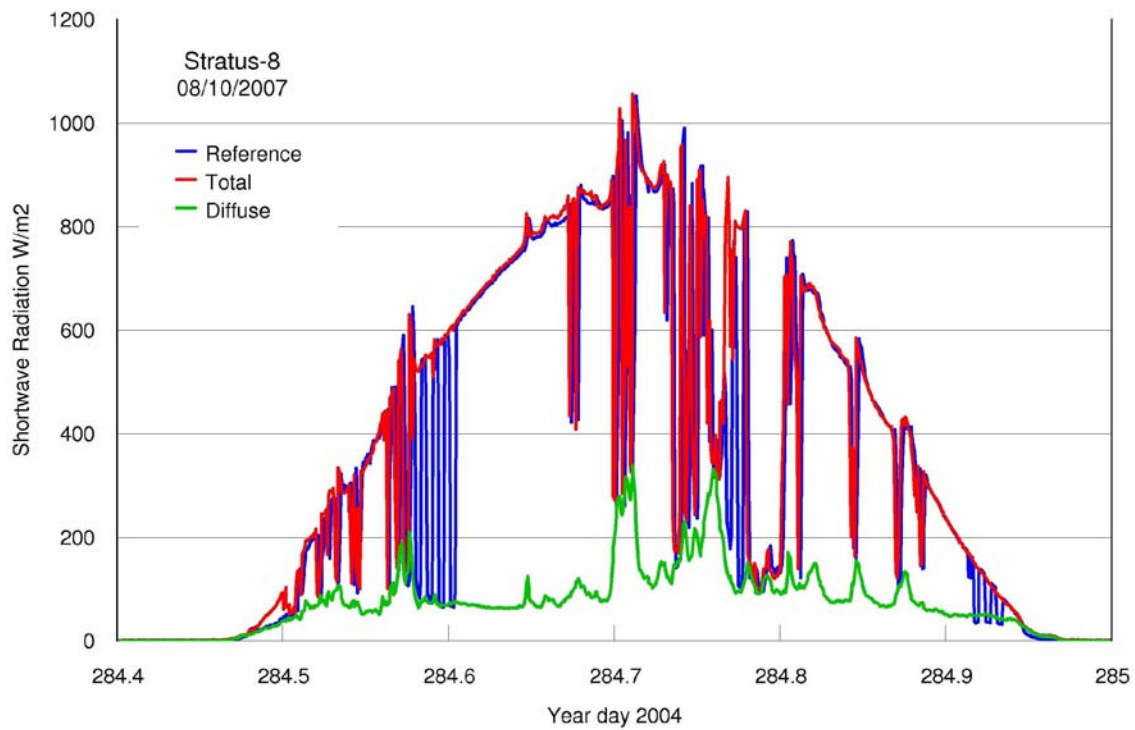


Figure 9. Time series of downward solar flux from a standard pyranometer (which measures total solar flux, i.e. the sum of direct and diffuse components) referred to as 'Reference' (blue line) and a total/diffuse system that measures the total solar flux (red line) and separately measures the diffuse solar flux component (green line) that results from scattering in the atmosphere. The diffuse component is small in clear skies but may be larger than the direct component under cloudy skies. The large excursions in the blue trace are caused by shading of the pyranometer from the sun's direct beam, which means the pyranometer indicates only the diffuse component.